

Supporting Information

Takahashi et al. 10.1073/pnas.1012582108

SI Text

Chromatin Immunoprecipitation (ChIP). To analyze Top1p–DNA complexes, Top1p was tagged at its C terminus with GFP-tag, and was expressed from its endogenous promoter and at its normal chromosomal loci. We performed two experiments to test whether Top1p-GFP is functional. We measured Top1p tagging impact on camptothecin sensitivity (Fig. S5). At 20 $\mu\text{g}/\text{mL}$ camptothecin, both wild type and Top1-GFP strain are mainly resistant to camptothecin indicating, that the tag does not enhance trapping on DNA. In an *srs2 Δ* background, which strongly sensitizes cells to camptothecin (1), Top1 tagging does not impact camptothecin sensitivity. In addition, we tested whether Top1-tagging influence the transcription associated mutagenesis which strongly depends on a functional Top1 (Table S2). In the *pGAL1-on* condition, the level of $-2/-3$ deletions is similar between the wild-type strain ($13.0e-7$) and the TOP1-GFP strain ($9.7e-7$). These two results indicate that the tagging of Top1 does not affect its ability to be trapped on DNA.

ChIP analyses were performed using modifications of (2). Experiments were realized starting from 100 mL of exponential growing cultures of BT46 (*pGAL1-CAN1*, *TOP1-GFP KanMX6*). Cells were grown in YP Glucose (*pGAL1-off*) or YP Galactose (*pGAL1-on*) until OD = 0.5–0.7. For camptothecin experiments, cells were grown in YP Glucose with 2% DMSO and with or without 20 $\mu\text{g}/\text{mL}$ camptothecin from OD = 0.2 to OD = 0.4–0.6. Cells were collected, successively washed in 20 mM Tris · HCl, pH8.0, and FA buffer (50 mM Hepes/150 mM NaCl/1 mM EDTA/1% Triton/0.1% sodium deoxycholate/0.1% SDS/1 mM AEBSF) and resuspended in 1 mL of FA buffer. An equal volume of glass beads (of diameter 0.5 mm) was added, and cells were disrupted by vortexing for 45 min at 4 °C. The lysate was diluted into 4 mL of FA buffer, and the glass beads were discarded. The crosslinked chromatin was pelleted by centrifugation at 17,000 $\times g$ for 20 min, resuspended in 800 μL of FA buffer for 1 h at 4 °C, and sonicated to yield an average DNA fragment size of 400 bp (range, 100–1,000 bp). Finally, the sample was adjusted to 1.6 mL with FA buffer, clarified by centrifugation at 10,000 $\times g$ for 30 min, and aliquots of the resultant chromatin solution were stored at -80 °C.

Chromatin solution (500 μL) was incubated with 5 μg of anti-GFP antibody (Roche Applied Science) coupled to 100 μL of Dynabeads anti-mouse IgG (DynaL Biotech ASA, Oslo, Norway). After 120 min at 21 °C on a rotator, beads were washed twice in 1 mL of FA buffer, once for 10 min in 0.5 mL of FA buffer with 500 mM NaCl, once in 0.5 mL of 10 mM Tris · HCl, pH 8.0/0.25 M LiCl/1 mM EDTA/0.5% N-P40/0.5% sodium deoxycholate, and once in 0.5 mL of TE (10 mM Tris · HCl, pH 8.0/1 mM EDTA). Immunoprecipitated material was eluted from the beads by heating for 20 min at 65 °C in 125 μL of 25 mM Tris · HCl, pH 7.5/5 mM EDTA/0.5% SDS, and then incubated at 37 °C in the presence of 1 mg/mL Pronase (Roche Applied Science). DNA was purified by using QIAquick PCR purification kit (Qiagen, Valencia, CA) and analyzed by quantitative PCR.

In all quantitative PCR experiments, immunoprecipitated DNA was normalized to input DNA, which corrects for differences in DNA amounts in samples from different experiments. Each 25 μL PCR mixture contained 12.5 μL of 2 \times Platinum SYBR Green qPCR Supermix-UDG (Invitrogen) 5 μL of diluted DNA template (either immunoprecipitated or input DNA), and 250 nM forward and reverse primers. All real-time PCR runs included a standard curve of 10-fold serial dilutions to calculate DNA mass in arbitrary units. The use of a standard curve allows the user to select only PCR data generated during a reaction with 80–100% efficiency. Real-time PCR quantitation was performed with each ChIP sample in duplicate and averaged to obtain a technical replicate value per sample to control for pipetting error.

PCR primers were designed to amplify ~ 200 bp at the following positions of the *CAN1* locus: 201–375, 520–689, 802–942, 1,108–1,294, and 1,566–1,733 bp. In addition, four primer couples were chosen outside the *CAN1* ORF, 458–209 bp upstream the start codon, and 150–325, and 565–758 downstream the stop codon. The primer sequences are available upon request.

Signals are expressed as the ratio between samples from galactose growth and glucose growth conditions or between 20 $\mu\text{g}/\text{mL}$ camptothecin-treated and untreated conditions. The data are presented as the mean of two biological replicate for camptothecin experiment and three biological replicates for the other experiment, with error bars representing 1 SEM.

1. Deng C, Brown JA, You D, Brown JM (2005) Multiple endonucleases function to repair covalent topoisomerase I complexes in *Saccharomyces cerevisiae*. *Genetics* 170:591–600.
2. Guglielmi B, Soutourina J, Esnault C, Werner M (2007) TFIIS elongation factor and Mediator act in conjunction during transcription initiation in vivo. *Proc Natl Acad Sci USA* 104:16062–16067.
3. Cassier-Chauvat C, Fabre F (1991) A similar defect in UV-induced mutagenesis conferred by the *rad6* and *rad18* mutations of *Saccharomyces cerevisiae*. *Mutat Res* 254:247–253.

4. Lebedeva N, Auffret Vander Kemp P, Bjornsti MA, Lavrik O, Boiteux S (2006) Trapping of DNA topoisomerase I on nick-containing DNA in cell free extracts of *Saccharomyces cerevisiae*. *DNA Repair (Amst)* 5:799–809.
5. Abousekhra A, Chanet R, Adjiri A, Fabre F (1992) Semidominant suppressors of *Srs2* helicase mutations of *Saccharomyces cerevisiae* map in the *RAD51* gene, whose sequence predicts a protein with similarities to prokaryotic RecA proteins. *Mol Cell Biol* 12:3224–3234.

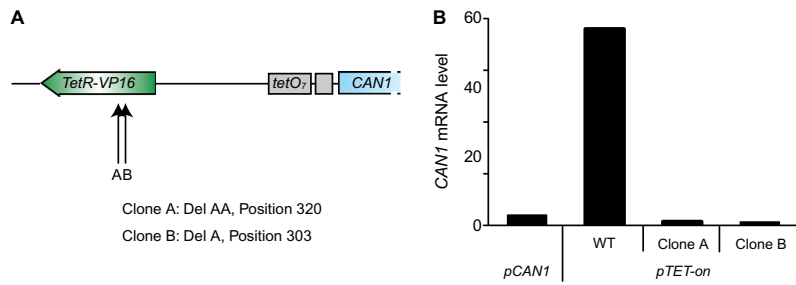


Fig. S1. Localization of Can^R mutations outside of *CAN1* ORF and consequence on *CAN1* transcription. (A) Schematic drawing of the *pTET-CAN1* construct. Arrows point to mutations observed in two Can^R clones (clone A and clone B) isolated under high transcription (*pTET-on*), which display no mutation inside the *CAN1* ORF. (B) Steady-state level of *CAN1* mRNA under high transcription (*pTET-on*) in wild-type, clone A, and clone B strains.

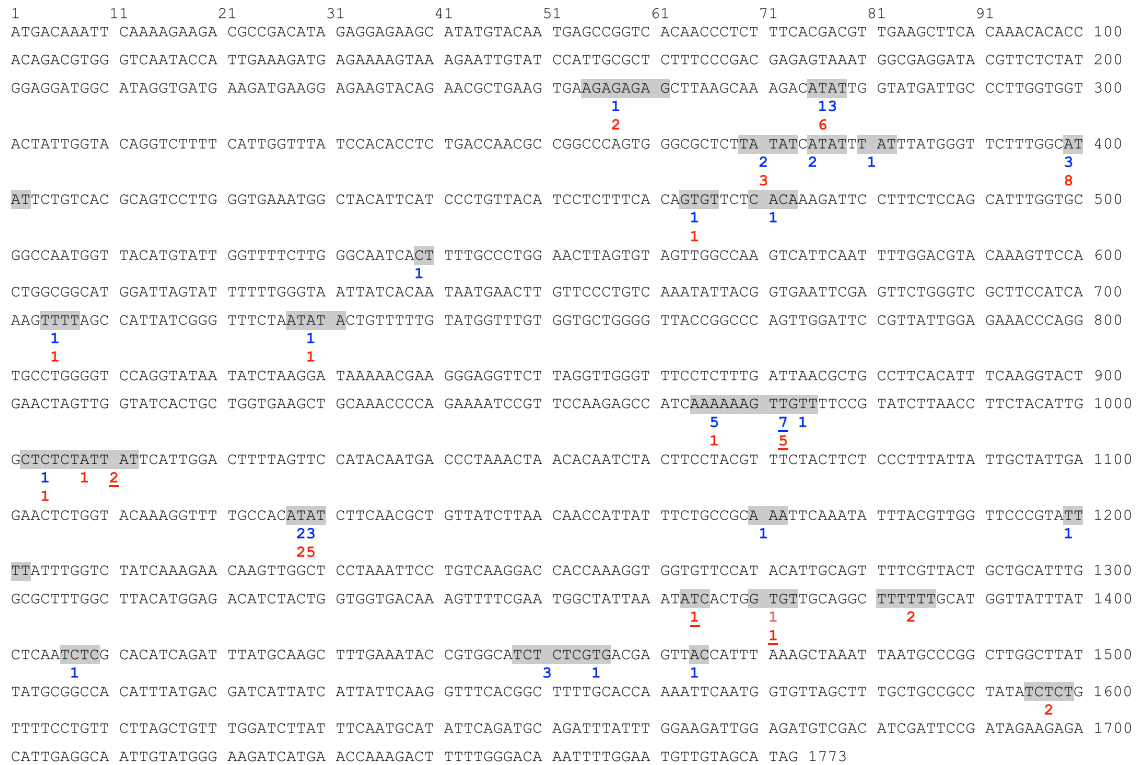


Fig. S2. Position of (–2)–(–3nt) deletions along the *CAN1* ORF (1–1773) in wild-type (blue) and *rev3Δ* (red) strains. Mutants were isolated under high transcription conditions (*pTET-on* and *pGAL1-on*). Values reported under the *CAN1* sequence indicate the number of mutations at a specific sequence position (boxed in gray). Underlined numbers point to (–3nt) events.

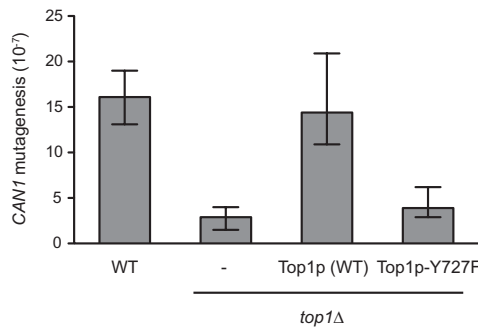


Fig. S3. *CAN1* spontaneous mutagenesis under high transcription (*pGAL1-on*) in a strain expressing the catalytically dead mutant Top1p-Y727F. Strains bearing a *TOP1* deletion were complemented by expressing a chromosome-integrated version of *TOP1-WT* or *top1-Y727F* placed under the control of its natural promoter and compared with wild-type and noncomplemented *top1Δ* strain. Strains are described in *Materials and Methods* and *Table S1*.

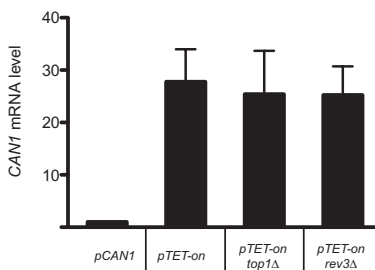


Fig. S4. Steady state level of *CAN1* mRNA under low (*pCAN1*) or high transcription (*pTET-on*) in wild-type, *top1* Δ , and *rev3* Δ strains. *CAN1* mRNA was quantified by RT-PCR from YPD exponential growing cultures. S.E.M. is represented.

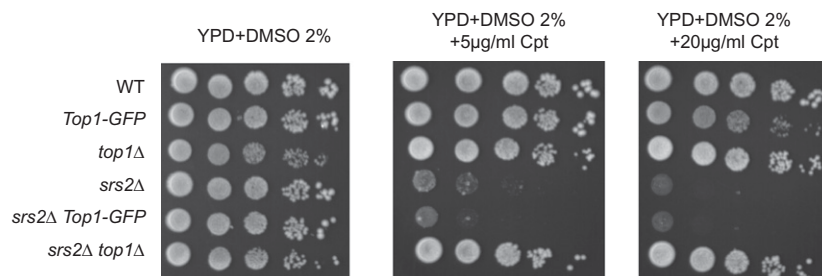


Fig. S5. Top1p-GFP impact on camptothecin sensitivity. The different strains were grown in liquid YPD for one day at 30 °C, diluted serially and spotted onto YPD plates containing DMSO 2% and 0, 5, and 20 μ g/mL camptothecin. For each strain, 50,000, 5,000, 500, 50, and 5 cells were spotted.

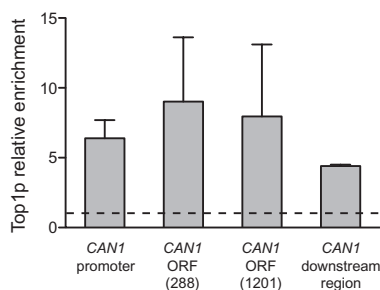


Fig. S6. Top1p-GFP enrichment on DNA after camptothecin exposure. Top1p-GFP recruitment is analyzed by ChIP in the *pGAL1-off* condition in 20 μ g/mL camptothecin-treated cells or in untreated cells. Histograms show the average signal ratio between treated and untreated cells. Top1p-GFP relative enrichment is measured inside *CAN1* promoter region, inside *CAN1* gene (position 288 bp and 1201 bp), and inside *CAN1* downstream region.

Table S1. List of strains used in this study

Strain name	Relevant genotype	Reference
FF18733	Wild type (<i>MATa</i> , <i>leu2-3-112</i> , <i>trp1-289</i> , <i>his7-2</i> , <i>ura3-52</i> , <i>lys1-1</i>)	3
BS144	FF18733 with <i>kanMX6/pTET-CAN1</i>	This study
BS199	FF18733 with <i>kanMX6/pGAL1-CAN1</i>	This study
BA1	FF18733 with <i>top1::kanMX6</i>	4
BS114	FF18733 with <i>can1::kanMX6</i>	This study
BT46	BS199 with <i>top1::kanMX6</i>	This study
BT30	BS199 with <i>rev3::URA3</i>	This study
BT64	BS199 with <i>tdp1::kanMX6</i>	This study
BT180	BS199 with <i>rad1::LEU2</i> , <i>mus81::kanMX6</i>	This study
BS174	BS144 with <i>top1::kanMX6</i>	This study
BS149	BS144 with <i>rev3::URA3</i>	This study
AC31	FF18733 with <i>TOP1-GFP kanMX6</i>	This study
BT185	BS199 with <i>TOP1-GFP kanMX6</i>	This study
FF18744	FF18733 with <i>srs2::LEU2</i>	5
BT16	FF18733 with <i>srs2::LEU2</i> , <i>TOP1-GFP kanMX6</i>	This study
BT56	FF18733 with <i>srs2::LEU2</i> , <i>top1::kanMX6</i>	This study
BT200*	BS199 with <i>top1::kanMX6</i> , <i>LEU2</i>	This study
BT201*	BS199 with <i>top1::kanMX6</i> , <i>LEU2 TOP1</i>	This study
BT202*	BS199 with <i>top1::kanMX6</i> , <i>LEU2 top1-Y727F</i>	This study

*Construction of strains BT200, BT201, and BT202 is detailed in *Materials and Methods* section.

